



## Climatic Zoning of South Khorasan Province in the Future Using General Circulation Models

Mahdi Amirabadizadeh<sup>a&d\*</sup>, Mohammad Puyafar<sup>b</sup>, Mostafa Yaghoobzadeh<sup>c&d</sup>

<sup>a</sup>Assistant Professor, Department of Water Engineering, University of Birjand, Birjand, Iran.

<sup>b</sup>MSc in Water Resources, Department of Water Engineering, University of Birjand, Birjand, Iran.

<sup>c</sup>Associate Professor, Department of Water Engineering, University of Birjand, Birjand, Iran.

<sup>d</sup>Research Group of Drought and Climate Change, University of Birjand, Birjand, Iran.

\*Corresponding Author, E-mail address: [mamirabadizadeh@birjand.ac.ir](mailto:mamirabadizadeh@birjand.ac.ir)

Received: 14 October 2023/ Revised: 06 December 2023/ Accepted: 29 December 2023

### Abstract

Climate is a complex system that is affected by changes in climatic parameters. By predicting and examining the range of changes in meteorological parameters in the future, it is possible to adopt appropriate solutions to reduce the harmful effects of climate change. Using atmospheric general circulation models is the most reliable method. In this study, precipitation, maximum and minimum temperatures of five synoptic stations of Birjand, Qaen, Nehbandan, Ferdows and Tabas, for the base period of 1988 to 2005 as well as the outputs of six climate models of CanESM2, GFDL-CM3, CSIRO-MK3, MPI-ESM - LR, MIROC-ESM and GISS-ES-R, were collected under RCP8.5 and RCP4.5 emission scenarios for a 16-year period (2020-2035) and downscaled using the LARS-WG5.0 model. Then, using the RMSE and MAE statistical indices, the quality of the down-scale representation was evaluated. Afterwards, by calculating the climate classification indices of De Martonne and Amberger, the province was classified with the help of GIS software. De Martonne classification indicates that the climate of the province will not change in the near future compared to the base period while based on the classification of Amberger and under all six models and both scenarios, Birjand, Qaen and Ferdows cities are predicted to have temperate climate and Tabas city is expected have a hot and mild desert climate. For Nehbandan city, the GFDL-CM3, CSIRO-MK3 and GISS-ES-R models of the fifth report under the RCP4.5 scenario predicted a moderate climate and the rest of the large-scale models predicted a moderate desert climate.

**Keywords:** Amberger, Climate change, De Martonne, Downscaling, South Khorasan Province.

### 1. Introduction

Climate change affects all climate-related ecosystems. These effects are divided into two general groups: biophysical and socio-economic. Biophysical effects include sea level rise, changes in ocean water salinity, sea temperature rise, changes in the quality of water and soil resources, increase in weeds and plant pests, and socio-economic effects include a decrease in agricultural production, fluctuations in world market prices, changes in industry and the economy, an increase in the risk of human hunger, food security intensification and finally migration (FAO, 2007; Delghandi, 2011).

One of the manifestations of climate change is the increase in temperature and the occurrence of temporal and spatial changes in rainfall. The mutual effects of these two phenomena will result in drought and flood. Drought, as one of the subtle natural disasters, is a situation of lack of rainfall and an increase in temperature that may occur in any climate. Drought is often described as a creeping, continuous phenomenon of the climate, which is associated with many financial and human losses. In addition to the socio-economic effects of climate change, drought has direct and indirect effects on the transformation of the natural environment.

Therefore, monitoring and investigating this phenomenon regarding climate change in the future will be the first step in recognizing and reducing the amount of its harmful damage. The more accurate this monitoring is, the more possible it will be to manage the dimensions of crises caused by and to compensate for their damages. The atmospheric General Circulation Models (GCM) is one of the most important tools available to evaluate the effects of climate change on a local and regional scale. These models predict the changes resulting from the effects of greenhouse gases on meteorological parameters.

In each geographical area, one or more climatic elements play a more significant role in shaping the climate of that place. Climatic zoning leads to the identification of zones that have similar climate. Climatic zoning is divided into two traditional and modern methods. Traditional classification methods are very diverse; however, common features can be found in all of them. The knowledge of different climates has attracted the attention of many scientists for a long time and has led to the invention of various climate classification methods such as Koppen, De Martonne, Ivanov, Amberger, Selianinov, Hans, etc., while the methods of Amberger and De Martonne have been used in this research.

Among the researches related to statistical downscaling methods one can refer to the study of Zarnistank et al. (2014) who reported a significant increase in temperature during spring and summer in Chaharmahal-Bakhtiari province in southwestern of Iran. The modeling results of their study showed that the temperature may increase between 1.69 and 6.88 °C by the year 2100. Also, the summer season may have a higher temperature increase than other seasons.

Through another research, Soltani and Hogenboom (2003) tested the climatic condition of Iran under the outputs of two AOGCM models, HadCM2 and ECHAM 4 and three emission scenarios from the IS92 emission scenarios by the MAGICC model. The results showed an increase of 1 to 1.5 °C in temperature and changes of -11 to +19 percent in rainfall under the low emission scenario. These studies showed that if the amount of gas emissions remains constant in

their current rate, it can cause an increase of 1.4-5 °C in temperature and changes of -30.9 to 50% in rainfall.

In another research, Rahimi et al. (2020) examined the future climate of Iran using data of 149 stations and output of 17 CMIP5 models. The results indicated that annual mean temperature is expected to increase significantly by 1.9 and 3.3 °C for the periods of 2041–2070 and 2071–2100, respectively. Also, computing climate types of Köppen–Geiger climate classification using averages from three climatic periods, indicated that the area of arid-desert and arid-steppe climate classes (BW and BS) and the area of moderate and snow climate classes (Ds and Cs) are expected to increase and decrease, respectively.

Bandari Khalafabadi et al. (2012) investigated these parameters in Khuzestan region with the aim of determining the number of changes in temperature and precipitation elements based on GCM model outputs. The large-scale model used by ECHO-G and the small-scale model by LARS-WG method were conducted under A1 scenario for three parameters of precipitation, minimum temperature and maximum temperature in eight synoptic stations of Khuzestan province. In this research, by examining the output of the model, it was determined that the study area has different reactions to climate change.

The results of the research showed that the maximum temperature decrease at Bostan station will be -1.8 °C and the maximum rainfall increase in Ramhormoz station will be 1.03 mm in the statistical period of 2010-2029. Also, in total, the eight studied stations will be associated with an increase in minimum temperature and a decrease in annual precipitation.

Allahvirdipour et al. (2023) evaluated the effects of climate change on climate classification in Iran. In this research, the data of 120 synoptic stations were used in the statistical period of 1993-2022. In order to investigate the effects of climate change in future periods, the output of the CanESM2 model from the CMIP5 model series was used under two RCP2.6 and RCP8.5 scenarios. The study of the climatic classification of Iran in the coming periods showed that most of the area of Iran will remain in dry and semi-arid

climate and the change in the climate class will not happen.

Hamed et.al (2023) studied the possible shift in climate zones in Southeast Asia (SEA) for different SSPs. The ability of 19 CMIP6 global climate models (GCMs) in reconstructing the Köppen-Geiger climate zones in SEA was analyzed using five categorical evaluation metrics. The best-performing models were selected to prepare an ensemble to project possible shifts in climate zones for different SSP scenarios in the future. Selected GCMs showed climate shifting in 3.4 to 12.6% of the total area of SEA for different SSPs. The highest geographical shift in climate was projected in the north, from dry winter and hot summer (Cwa) to tropical with dry winter (Aw), followed by Aw to tropical monsoon (Am) in the north and south, and tropical without dry season (Af) to Am in the middle and southwest of SEA.

Peel et al. (2006) classified the world's climate based on the Köppen-Keiger classification, and finally the world's climate was divided into five climate zones with the new Köppen-Keiger classification, and in this method, separate borders were considered for the climates. But again, multivariate methods provide better results. In Iran, studies have been conducted in the field of climate classification.

In research of modern statistical methods and GIS, the climatic zoning of Sistan and Baluchistan province was done with different statistical software and the climate of the province was divided into five regions by the clustering method, and the clustering method was declared to be the best method in this research (Salighi et al., 2017).

Climatic zoning of central province was also done using factor and cluster analysis and seven different climatic zones were identified using factor analysis and finally by cluster analysis. The results of the research showed seven different climate zones, including the temperate and humid dusty, hot and semi-arid, semi-cold and semi-humid dusty, temperate and semi-arid dusty, temperate dry mime, cold and semi-arid dusty, and semi-cold and dry dusty areas. Khosravi and Armesh, (2011).

Taghvi et al. (2010) presented climate zoning for 65 synoptic stations of the country using spectral analysis and clustering. The

climatic indicators used included 24-hour daily maximum precipitation, daily maximum and minimum temperature, as well as the time series of climatic data related to the period of 1986 to 2005. Based on their results, Torbat-Heydarieh station was placed in one climatic zone and Sabzevar, Sarakhs and Mashhad stations were placed in another climatic station.

Mohammad Lo and Tahmasbipour (2016) also evaluated the effects of climate change on climate classifications in two stations of Urmia and Khoy in the base period (1979-2009). The climatic classifications of De Martonne and Selianinov were used in this research. The results showed that under the influence of climate change at Urmia station, De Martonne aridity coefficient will have an increasing trend and the climate type will move from semi-arid type in the base period to Mediterranean climate in the future period.

According to the climate classification of Selianinov, the climate of the region will shift from dry steppe to humid steppe. At Khoy station, according to the climate classification of De Martonne, under the influence of climate change, the climate coefficient of De Martonne decreases and the area becomes drier.

Abbasi et al. (2010) predicted climate changes in South Khorasan province between 2010 and 2039 using the statistical downscale output of the ECHO-G model. The data of ECHO-G general circulation model to evaluate the climate change and drought and frost in South Khorasan province was downscaled with LARS-WG model and the general results of the survey in the given period indicated a 4% increase in precipitation, a decrease in the number of frost days and an increase in the annual average which was around 0.3°C and the highest daily increase in temperature was predicted to be 1°C in winter season.

Based on the comprehensive literature review performed, the effects of global warming on the climate of the entire South Khorasan province have not been studied yet and in some cases, only specific stations have been chosen. Therefore, in this research, by using observational data at 5 meteorological stations in the South Khorasan province and the output of six ocean-atmosphere general circulation models with three emission scenarios, the climatic condition of the given

province is investigated for the near future. Moreover, the climate classification was done using De Martonne and Amberger indices.

## 2. Materials and Methods

### 2.1. Study area

South Khorasan province is located in the eastern part of Iran, between  $57^{\circ} 46'$  to  $57^{\circ} 60'$  East longitude and  $34^{\circ} 14'$  to  $35^{\circ} 30'$  North latitude, centered on the city of Birjand. This province is located in the dry and semi-arid climate belt of the planet and its distance from

the sea and its proximity to the salt desert, Lut, and extra-regional winds such as the 120-day wind of Sistan have exacerbated the dryness of the air in this region. The area of this province is 150,800 square kilometers, which includes four watersheds of Lut desert, Markazi desert, Khaf and Hamoon. Despite such a large area, only five synoptic stations (Ferdows, Qaen, Birjand, Nehbandan and Tabas (Figure 1)) are located in the province which have relatively long-term statistics for climate studies being used in this research.

**Table 1.** Characteristics of the studied synoptic stations

Station	Longitude (East)	Latitude (North)	Height above mean sea level (m)
Birjand	$59^{\circ} 12'$	$32^{\circ} 52'$	1491
Tabas	$55^{\circ} 56'$	$36^{\circ} 33'$	711
Qaen	$59^{\circ} 10'$	$33^{\circ} 43'$	1432
Nehbandan	$60^{\circ} 02'$	$31^{\circ} 54'$	1188
Ferdows	$58^{\circ} 11'$	$34^{\circ} 02'$	1293

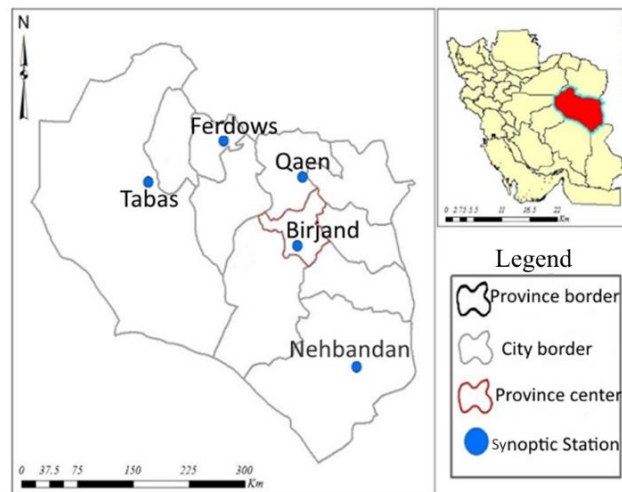


**Fig. 1.** The locations of South Khorasan Province in Iran and synoptic stations in the province

The data used in this research include two groups, observational data and data extracted from six GCM models related to the fifth climate change report. The daily observational data are related to minimum temperature,

maximum temperature and precipitation which are collected from five synoptic stations of Birjand, Qaen, Tabas, Ferdows and Nehbandan within 1988-2017.

**Table 2.** Statistical characteristics of rainfall (mm) in the investigated stations

Station	Daily rainfall (mm)		Maximum temperature(C°)		Minimum temperature(C°)	
	Mean	Standard deviation	Mean	Standard deviation	Mean	Standard deviation
Birjand	0.46	0.15	24.6	9.52	8.40	8.56
Tabas	0.48	0.28	22.3	9.3	6.33	8.10
Qaen	0.22	0.39	28.95	10.67	14.20	9.65
Nehbandan	0.40	0.4	26.9	9.30	12.80	9.30
Ferdows	0.37	0.93	24.51	10.2	10.55	8.80

After the qualitative review of the observational data of the given stations, the output of six large-scale climate models, which are shown in Table (3), were downloaded from

the following source: [https://gdo-dcp.ucllnl.org/downscaled\\_cmip\\_projections/dcpInterface.html#Projections:%20Complete%20Archives](https://gdo-dcp.ucllnl.org/downscaled_cmip_projections/dcpInterface.html#Projections:%20Complete%20Archives)

For the time period of 2020-2035, precipitation data, maximum temperature and minimum temperature, under two scenarios of the fifth report i.e., RCP4.5 and RCP8.5, were extracted from GCMs models listed in Table 3. One of the major problems in using the outputs

of atmospheric general circulation models (GCMs) is the large scale of their computational cells in terms of space compared to the studied area (Kilsby and Jones 2007).

**Table 3.** Large-scale models of the fifth report used in this research

row	Model	Manufacturer	Related institution
1	CanESM2	Canada	Center for Climatic Survey and Modeling
2	GFDL-CM3	America	Geophysical Fluid Dynamics Laboratory
3	CSIRO-MK3	Australia	Atmospheric Research CSIRO
4	MPI-ESM-LR	Germany	Max Planck Institute for Meteorology
5	MIROC-ESM	Japan	Pacific Research Institute, National Institute for Environmental Studies, Japan Marine Science and Industry Agency and Japan Technology
6	GISS-ES-R	America	NASA Space Studies Institute

To overcome the lack of spatial resolution of general circulation models, there are two solutions: statistical downscaling representation using statistical models and the use of regional dynamic models (Babaian et al., 2010). In this research, the LARS-WG5.0 software was used as the statistical downscaling method.

## 2.2. LARS-WG5.0 model

This model was designed and developed by Mikhail Semenov at Long Ashton Research Station. LARS-WG is a random weather generator that is used to simulate the weather of a site in both current and future weather conditions. This multivariate regression model uses statistical techniques to generate weather data. Also, due to the repetition of calculations, it requires fewer input data and is simpler to use than other models (Semenov et al., 1997). This model could simulate the past and future periods, but for any modeling, a special climate scenario is required. This model can be used to model missing data and statistical gaps.

## 2.3. Evaluation criteria

In this research, in order to evaluate the results of the statistical downscale method and for the climatic parameters of maximum and minimum temperatures and precipitation, the statistical measures of root mean square error, mean absolute error, and determination coefficient were used:

$$RMSE = \sqrt{\frac{\sum_{i=1}^n (x_i - x_m)^2}{n}} \quad (1)$$

$$MAE = \frac{\sum_{i=1}^n |x_i - x_m|}{n} \quad (2)$$

$$R^2 = \frac{\sum_{i=1}^n (x_m - \bar{x}_m)^2}{\sum_{i=1}^n (x_i - \bar{x}_m)^2} \quad (3)$$

where,  $x_i$ : downscaled values,  $x_m$ : observational values (observed) and  $n$ : total number of observations. The value of RMSE is always positive and the closer it is to zero, the more accurate the model is in simulating the investigated variable. The MAE index expresses the accuracy of the model. As its value increases, the accuracy of the model decreases and vice versa. The  $R^2$  value varies from zero to one and as it approaches one, it shows the data are better fitted.

In this research, two greenhouse gas emission scenarios of RCP4.5 and RCP8.5, belonging to CMIP5, which show average and pessimistic scenarios, respectively, were used. In the RCP4.5 scenario presented by the MiniCAM modeling group; the amount of radiate forcing caused by the concentration of greenhouse gases will remain constant at 4.5 watts per square meter until the end of the year 2100.

On the other hand, in the RCP8.5 scenario, which is a pessimistic scenario, no policy will be implemented to reduce the concentration of greenhouse gases until the year 2100 and therefore the amount of radiate forcing will be 8.5 watts per square meter until the end of this year.

In this research, the two methods of De Martonne and Amberger were used to classify

the province climate while the details of which are presented in the following sections.

#### 2.4. De Martonne climate classification

In this method, annual temperature and precipitation are the bases for calculating the humidity index and by using this method and based on the different values obtained for the index (I), climates are distinguished from each other. The coefficient of dryness (I) is obtained from the following equation:

$$I = \frac{P}{T + 10} \quad (4)$$

where, p is the average annual rainfall in millimeters and T is the average annual temperature in degrees Celsius. Table 4 shows the range of dryness coefficient for each of the six classes.

**Table 4.** Range of I value for each of the six climate classes

Name of the climate	Range of De Martonne aridity factor (I)
Dry	$I < 10$
Semi-arid	$10 < I < 19$
Mediterranean	$20 < I < 23.9$
Semi-humid	$24 < I < 27.9$
Wet	$28 < I < 34.9$
Very humid	$I > 35$

#### 2.5. Amberger classification

In the Ambergis classification method, the determining factors of the climate in each region are the average maximum temperature in the hottest month of the year (M), the average minimum temperature in the coldest month of the year (m) and the average annual

rainfall (P), which based on this method, thirteen different climates can be defined. In this method, a diagram is used for climate classification where the horizontal axis is the value of m in degree centigrade and the vertical axis is the value of  $Q_2$  whose value is determined from the following formula:

$$Q_2 = \frac{2000P}{m^2 - M^2} \quad (5)$$

### 3. Results and Discussion

In order to determine the climatic condition of the cities of the province in the base period, the data obtained from five aforementioned synoptic stations were used. The results of climate determination according to De Martonne and Amberger indices are shown in Table 5.

According to the calculations made for the base period data in the De Martonne classification, five synoptic stations of the province are located in the dry climate and based on the classification of Amberger, Birjand, Qaen, Nehbandan and Ferdows were located in the cold dry climate and Tabas in the hot mild desert climate. In order to determine the climate of the province in the near future, first the data of precipitation, maximum temperature and minimum temperature under the two scenarios RCP8.5 and RCP4.5 were obtained from the outputs of the six large-scale models that were introduced earlier (Table 3), then with the assistance of the LARS-model WG, the data were downscaled.

**Table 5.** Determining the climate of the base period based on De Martonne and Amberger indices

Name of The City	Index of De Martonne (I)	Type of Climate	Index of Amberger ( $Q_2$ )	Type of Climate
Birjand	6.38	dry	15.25	dry cold
Qaen	7.59	dry	17.33	dry cold
Nehbandan	4.70	dry	17.72	dry cold
Ferdows	5.44	dry	13.41	dry cold
Tabas	2.67	dry	7.47	mild hot desert

#### 3.1. Evaluation results of the representative downscaling model

The evaluation results of the LARS-WG model for precipitation parameters, maximum temperature and minimum temperature in the discussed synoptic stations are described below.  $R^2$ , RMSE and MAE indices were used for evaluation.

Using the weighting method, the performance of these six models was

determined based on the simultaneous consideration of each of the three evaluation indices and the weight of each was determined. Therefore, the model with the highest weight will have the highest rank in the final evaluation and the model with the lowest weight will have the lowest rank. The index values and ranks of the GCMs are provided in Table 6 through Table 11 for different variables and stations.

As shown in table 6 and 7, in the downscaling of monthly precipitation variables, the first performance rank at five stations was related to the CSIRO-MK3, MIROC-ESM, and CanESM2 models. The

best performance in downscaling of maximum temperature at five stations was related to CSIRO-MK3 and MIROC-ESM models (Table 8 and Table 9).

**Table 6.** Statistical evaluation of LARS-WG model for precipitation data. (The RMSE and MAE are in mm)

MODEL	Birjand				Qaen				Nehbandan			
	RMSE	MAE	R <sup>2</sup>	Rank	RMSE	MAE	R <sup>2</sup>	Rank	RMSE	MAE	R <sup>2</sup>	Rank
CanESM2	0.63	0.37	0.33	3	0.7	0.41	0.34	2	0.72	0.36	0.28	1
GFDL-CM3	0.72	0.41	0.20	5	0.86	0.49	0.14	6	0.9	0.44	0.07	5
CSIRO-MK3	0.59	0.33	0.40	1	0.71	0.4	0.32	3	0.8	0.4	0.17	2
MPI-ESM-LR	0.7	0.42	0.23	4	0.79	0.47	0.21	4	0.84	0.41	0.13	4
MIROC-ESM	0.6	0.34	0.38	2	0.7	0.39	0.32	1	0.82	0.4	0.15	3
GISS-ES-R	0.76	0.45	0.15	6	0.81	0.47	0.18	5	0.91	0.44	0.07	6

**Table 7.** Statistical evaluation of LARS-WG model for precipitation data. (The RMSE and MAE are in mm)

Model	Ferdows				Tabas			
	RMSE	MAE	R <sup>2</sup>	Rank	RMSE	MAE	R <sup>2</sup>	Rank
CanESM2	0.68	0.4	0.17	2	0.42	0.23	0.18	3
GFDL-CM3	0.72	0.41	0.12	4	0.44	0.23	0.14	5
CSIRO-MK3	0.65	0.36	0.23	1	0.37	0.2	0.30	1
MPI-ESM-LR	0.73	0.42	0.11	5	0.45	0.23	0.12	6
MIROC-ESM	0.65	0.35	0.22	1	0.4	0.22	0.24	2
GISS-ES-R	0.69	0.4	0.17	3	0.43	0.23	0.17	4

**Table 8.** Statistical evaluation of LARS-WG model for maximum temperature data. (The RMSE and MAE are in °C)

Model	Birjand				Qaen				Nehbandan			
	RMSE	MAE	R <sup>2</sup>	Rank	RMSE	MAE	R <sup>2</sup>	Rank	RMSE	MAE	R <sup>2</sup>	Rank
CanESM2	2.58	1.99	0.92	4	2.54	1.95	0.91	4	2.47	1.92	0.93	4
GFDL-CM3	2.47	1.91	0.92	3	2.54	1.94	0.91	3	2.43	1.87	0.93	3
CSIRO-MK3	2.32	1.78	0.93	1	2.42	1.83	0.92	1	2.34	1.79	0.94	2
MPI-ESM-LR	2.63	1.96	0.91	5	2.7	2.0	0.90	6	2.67	2.0	0.92	6
MIROC-ESM	2.422	1.86	0.93	2	2.51	1.89	0.92	2	2.32	1.79	0.94	1
GISS-ES-R	2.63	2.1	0.91	6	2.62	2.9	0.91	5	2.52	2.02	0.93	5

**Table 9.** Statistical evaluation of LARS-WG model for maximum temperature data. (The RMSE and MAE are in °C)

Model	Ferdows				Tabas			
	RMSE	MAE	R <sup>2</sup>	Rank	RMSE	MAE	R <sup>2</sup>	Rank
CanESM2	2.57	1.95	0.93	4	2.62	1.97	0.94	4
GFDL-CM3	2.54	1.93	0.93	3	2.54	1.94	0.94	2
CSIRO-MK3	2.45	1.87	0.94	1	2.48	1.91	0.94	1
MPI-ESM-LR	2.71	2.4	0.92	6	2.67	2.4	0.93	6
MIROC-ESM	2.49	1.91	0.93	2	2.54	1.99	0.94	3
GISS-ES-R	2.62	2.14	0.93	5	2.7	2.16	0.94	5

**Table 10.** Statistical evaluation of LARS-WG model for minimum temperature data. (The RMSE and MAE are in °C)

Model	Birjand				Qaen				Nehbandan			
	RMSE	MAE	R <sup>2</sup>	Rank	RMSE	MAE	R <sup>2</sup>	Rank	RMSE	MAE	R <sup>2</sup>	Rank
CanESM2	2.02	1.62	0.93	1	2.37	1.87	0.91	5	1.94	1.57	0.95	1
GFDL-CM3	2.05	1.7	0.93	2	2.34	1.81	0.91	1	2.02	1.61	0.95	2
CSIRO-MK3	2.07	1.65	0.93	3	2.36	1.81	0.91	2	2.14	1.67	0.94	4
MPI-ESM-LR	2.11	1.7	0.93	4	2.42	1.87	0.90	4	2.16	1.74	0.94	4
MIROC-ESM	2.05	1.72	0.94	3	2.37	1.83	0.91	4	2.03	1.63	0.95	3
GISS-ES-R	2.06	1.7	0.93	3	2.35	1.85	0.91	3	2.14	1.69	0.94	5

**Table 11.** Statistical evaluation of LARS-WG model for minimum temperature data. (The RMSE and MAE are in °C)

Model	Ferdows				Tabas			
	RMSE	MAE	R <sup>2</sup>	Rank	RMSE	MAE	R <sup>2</sup>	Rank
CanESM2	1.92	1.54	0.94	3	2.01	1.58	0.95	1
GFDL-CM3	1.86	1.52	0.95	1	2.10	1.66	0.95	3
CSIRO-MK3	2.01	1.59	0.94	6	2.09	1.63	0.95	2
MPI-ESM-LR	1.96	1.54	0.94	4	2.11	1.65	0.95	4
MIROC-ESM	2.0	1.56	0.94	5	2.14	1.68	0.95	5
GISS-ES-R	1.91	1.54	0.94	2	2.14	1.72	0.95	6

The results of ranking of six GCM models in downscaling of minimum temperature at five stations of South Khorasan Province showed that CanESM2, GFDL-CM3 are ranked first (Table 10 and Table 11). Also, the downscaling results of three climatic parameters using the LARS-WG method showed that models GISS-ES-R and MPI-ESM-LR were not ranked in priority at any of the five stations of the province.

Based on the downscaling results of the data for all the stations studied, the CanESM2 and GFDL-CM3 models showed the highest average amount of rainfall and maximum temperature, respectively (Figure 2 to Figure 4). The CSIRO-MK3 model also brought about the lowest average temperature of the committee. Also, all the large-scale models showed an increase in precipitation and temperature for the province which is

consistent with the study of Abbasi et al. (2009). As shown in Figure 2 through Figure 4, the CanESM2 and MPI-ESM-LR models predicted an increase in precipitation, minimum temperature and maximum temperature for RCP8.5 in comparison to RCP4.5 scenario.

### 3.2. Estimation of climatic indicators in the near future period

The results of the simulation of changes in the climate indices of De Martonne and Amberger, affected by the climate change phenomenon, are brought in figure 5. It is worth mentioning that the given figure is for the near future horizon, including cities of Birjand, Qaen, Nehbandan, Ferdows and Tabas, under the two scenarios RCP4.5 and RCP8.5 being compared the base period.

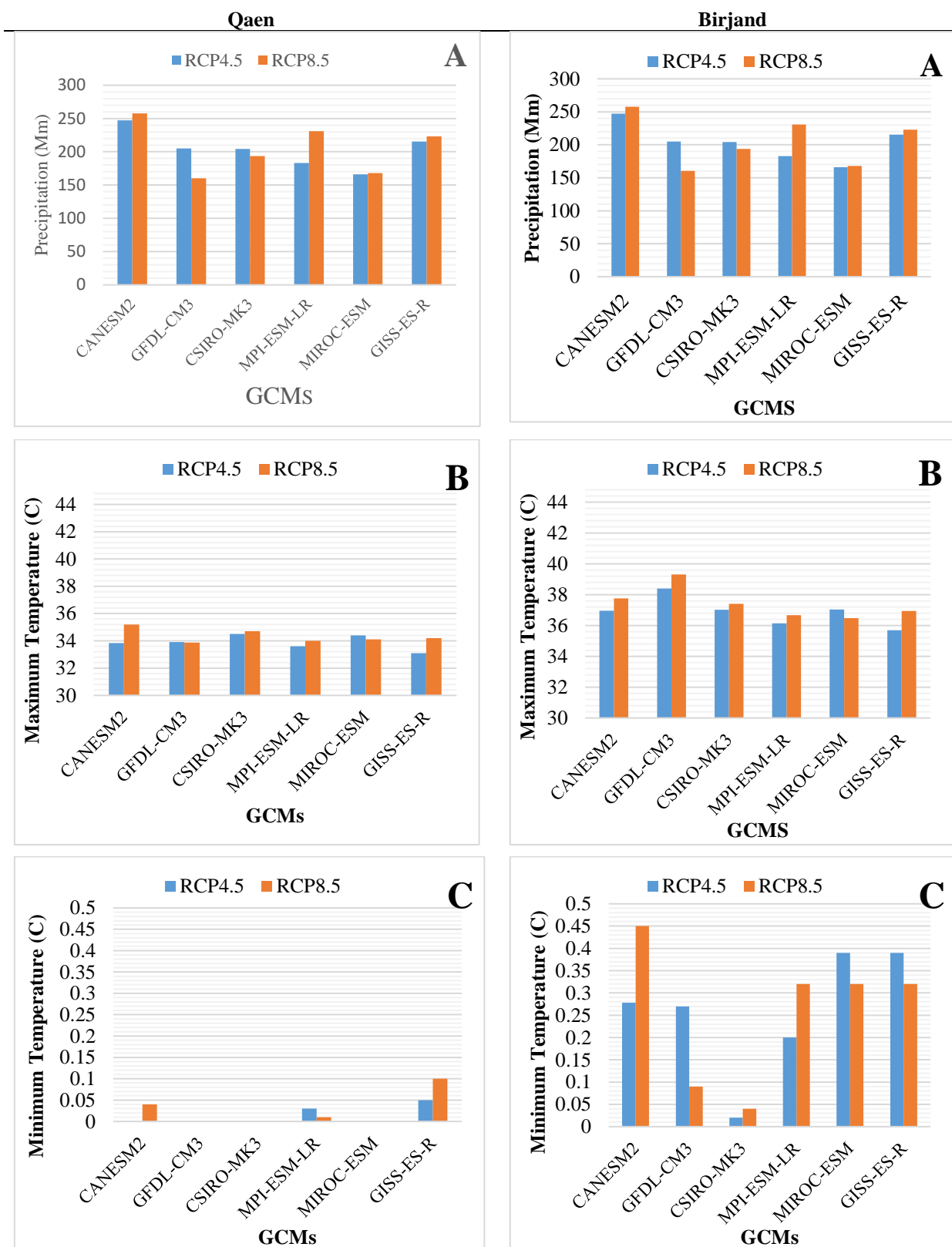


Fig. 2. Downscaling results of Birjand and Qaen city data

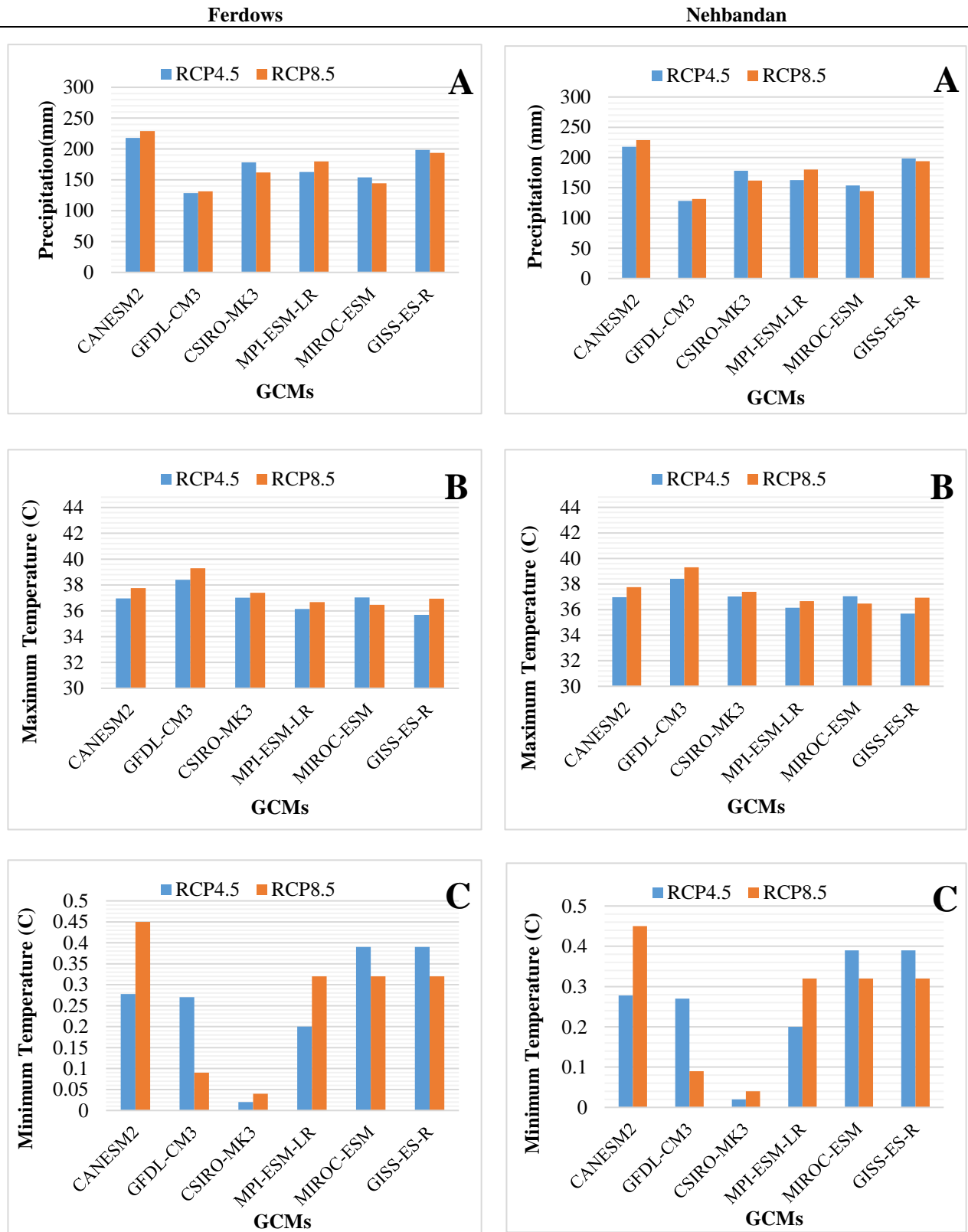
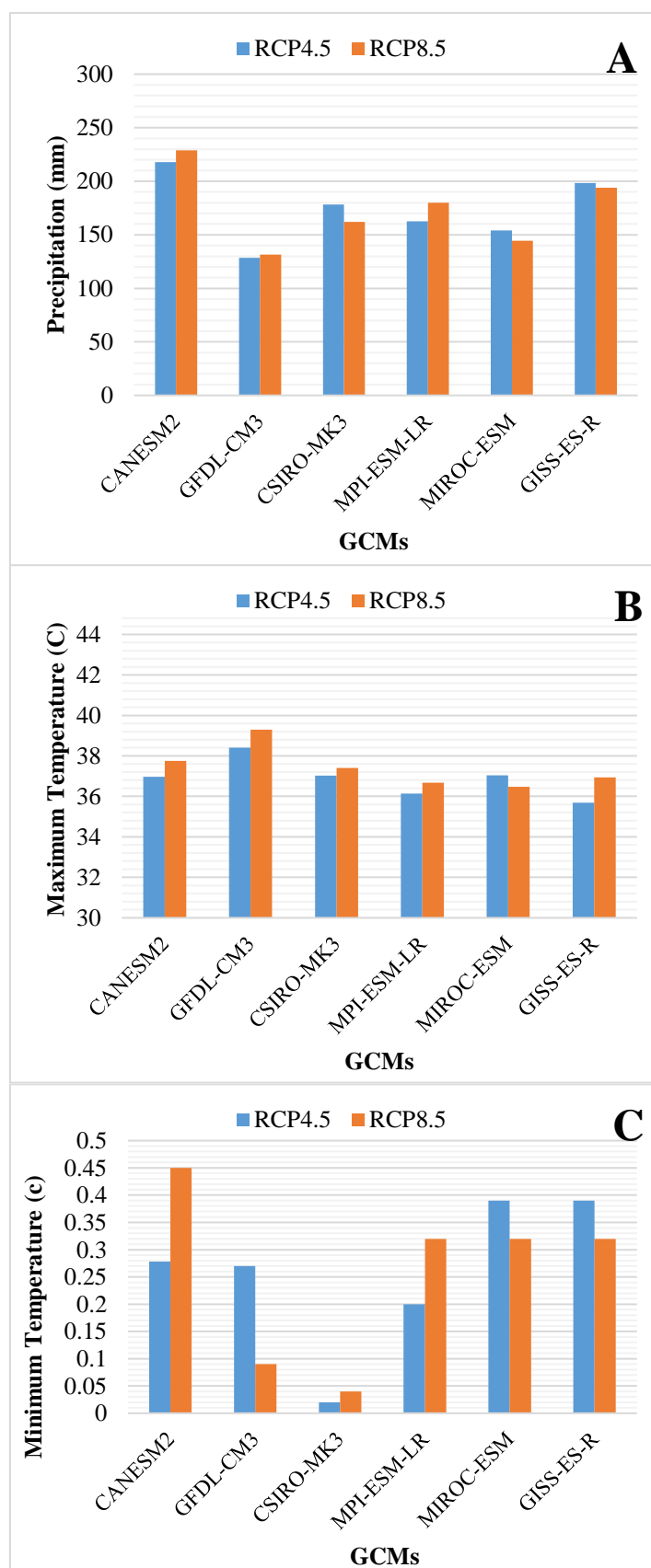


Fig. 3. Downscaling results of the data of Nehbandan and Ferdows cities



**Fig. 4.** Downscaling results of precipitation data (A), maximum temperature (B) and minimum temperature (C) in Tabas city



**Fig. 5.** Values of De Martonne and Amberger indices in the near future compared to the base period

As can be seen in Figure 5, in Birjand city, the CanESM2 model has estimated a higher De Martonne and Amberger indices value compared to other models and on the other hand, the GFDL-CM3 model provided the lowest estimate. Also, GFDL-CM3 and

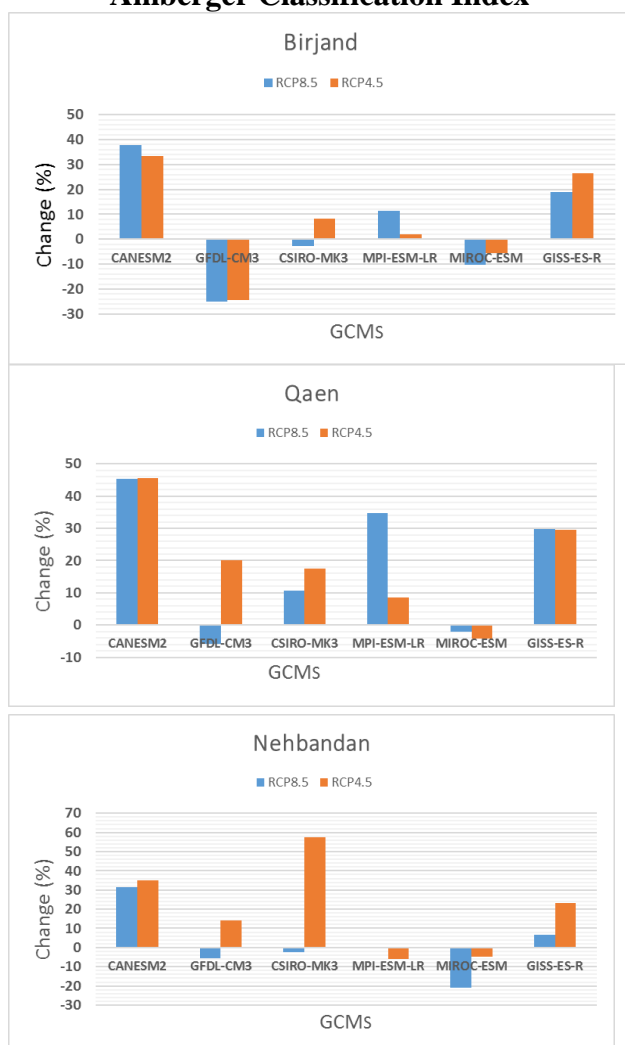
MIROC-ESM models showed that the values of the indices for the near future, in comparison to the value of the base period, were lower while other large-scale models showed higher values. In Qaen city, like Birjand station, the CanESM2 model estimated a higher De

Martonne and Amberger values compared to other models and the MIROC-ESM model led to the lowest estimate. Moreover, the MIROC-ESM model showed that the value of the index for the near future period is lower than that of the base period. In Nehbandan city, the CSIRO-MK3 model, compared to other models, estimated a higher value of the De Martonne and Amberger indices while the MIROC-ESM model brought about the lowest estimate. Furthermore, the MPI-ESM-LR and MIROC-ESM models also showed that the value of the index for the near future period is lower than that of the base period while other large-scale models indicated higher values. In the cities of Ferdows and Tabas, CanESM2 model approximated higher De Martonne and Amberger index values, in comparison to other models and the GFDL-CM3 model also provided the lowest estimate. Finally, the

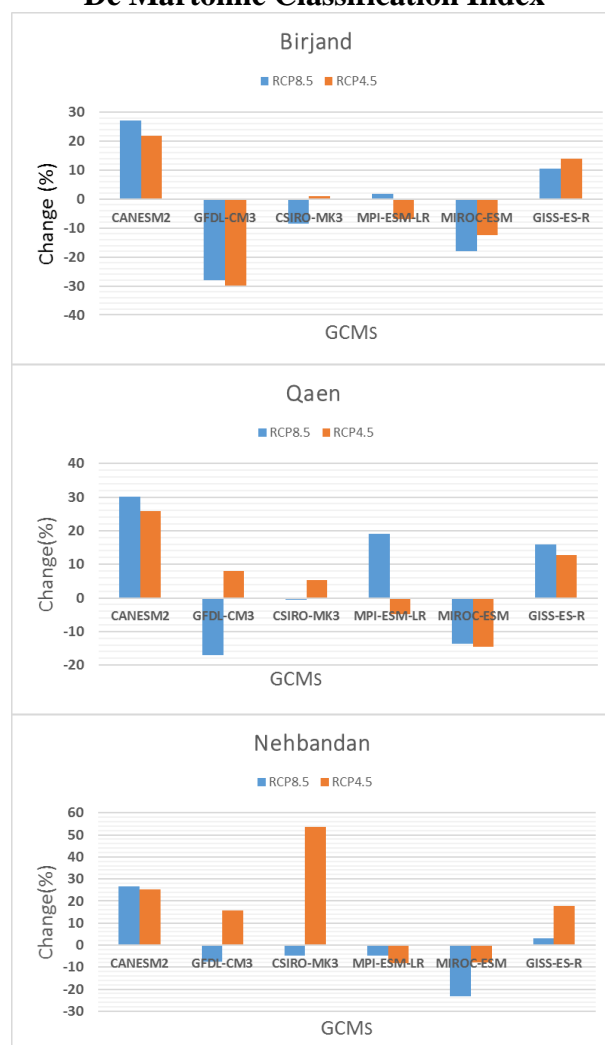
CSIRO-MK3 and MIROC-ESM models specified that the value of the index for the near future period is lower than that of the base period.

The percentage of changes in climatic indicators used in this research in the near future period compared to the base period is shown in the figure below. As seen in Figure 6, the CanESM2 and GFDL-CM3 models showed the highest and the least percentage of changes in most of the weather stations, based on the two studied scenarios, compared to the base, respectively. This percentage of changes in the models is estimated between -30% and 58% in different scenarios compared to the base period. Despite this range of changes in this statistical parameter, the climatic classification of South Khorasan Province has become closer to the borders of becoming a newer climatic classification.

### Amberger Classification Index



### De Martonne Classification Index



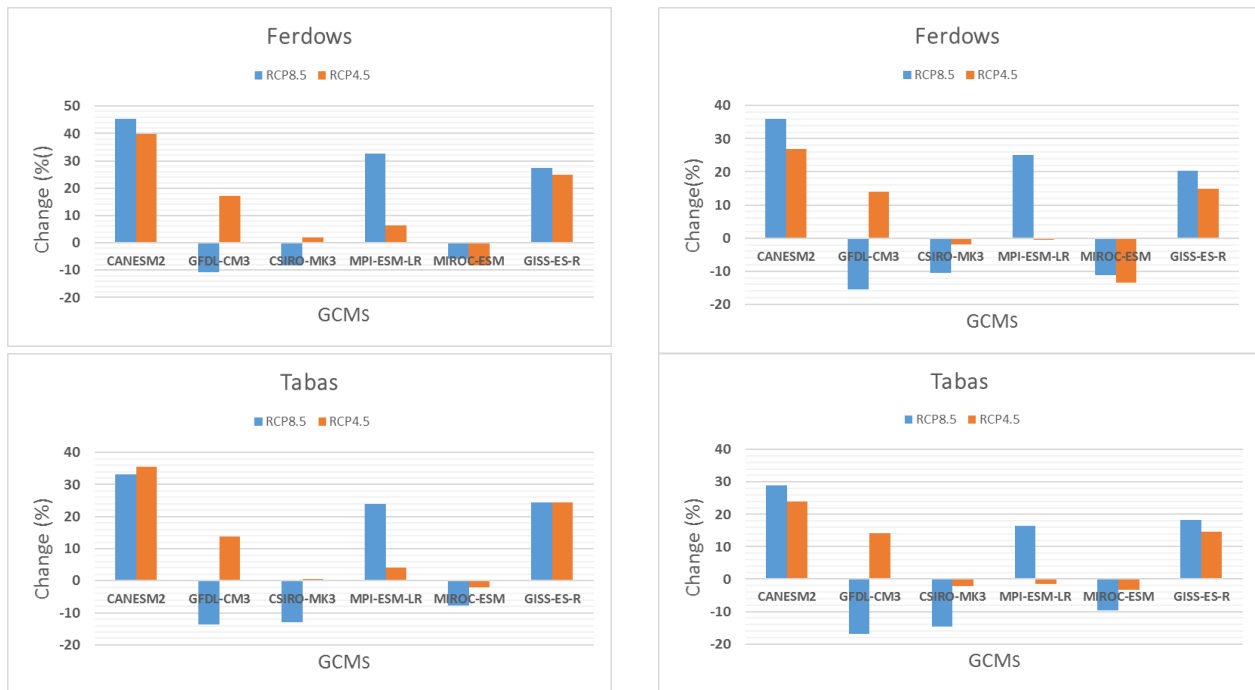


**Fig. 6.** The percentage of changes in the De Martonne and Amberger indexes in the near future compared to the base period

#### 4. Conclusion

The purpose of this research is to investigate the climatic condition of South Khorasan Province in the near future using the output of six climate models and two greenhouse gas emission scenarios. To this end, the data of precipitation, maximum and minimum temperatures of five synoptic stations including Birjand, Qaen, Nahbandan, Ferdows and Tabas and also De Martonne and Amberger climatic classification indices were used. The obtained results showed that for all six models considered, under the two above-mentioned released scenarios, all the five studied cities will be located in dry climate according to De Martonne classification, which indicates that the climate of the province will not change in the near future compared to the base period. Also, the results showed that the De Martonne index value is closer to the border of the semi-arid layer (the values of De Martonne index will increase in the near future). These results are in consistent with the results of research conducted by Mohammadlu and Tahmasbipour (2016).

In the classification of Amberger, Birjand, Qaen and Ferdows are in moderate climate for all six models and under both scenarios while Tabas city is located in a mild hot desert climate. For Nahbandan city, GFDL-CM3, CSIRO-MK3, and GISS-ES-R models under

RCP4.5 scenario indicated a temperate climate and the rest of GCM's models showed temperate desert climate.

The output results of the CanESM2 model indicated more positive values of the De Martonne index and coefficient of variation. Also, this model showed more rainfall in the near future compared to the base period and other GCMs. This result is in consistent with the results of research performed by Allahverdipour et al. (2023) in which they predict an increase in precipitation value in near future. In comparison to other models, the GFDL-CM3 model predicted the highest maximum temperature and the lowest minimum temperature with regard to the CSIRO-MK3 model.

#### 5. Disclosure Statement

No potential conflict of interest was reported by the authors.

#### 6. References

- Abassi, F., Malbusi, S., Babaeian, I., Asmari, M., & Borhani, R. (2010). Climate change prediction of south Khorasan Province During 2010-2039 by using statistical Downscaling of ECHO-G Data. *Water and Soil*, 24(2).
- Allahverdipour, P., Ghorbani, M. A., & Asadi, E. (2023). Evaluating the effects of climate change on the climatic classification in Iran. *Water and*

*Soil Management and Modelling*, (in press), -. doi: 10.22098/mmws.2023.12755.1271

Babaian, I., Najafinik, Z., Zabol Abbasi, F., Habibi Nokhandan, M., Adab, H., & Malboosi, S. (2009). Assessing the country's climate change in the period of 2010-2039 using the exponential downscale data of ECHOG atmospheric general circulation model. *Journal of Geography and Development*, 7(16), 152-135.

Bandari Khalafabadi, V., Shakiba, A., & Azimi, F. (2012). Prediction of precipitation regime and temperature in Khuzestan with atmospheric general circulation models. *Journal of Natural Geography*, 6(19), 59-70.

Delghandi, M. (2011). Investigating the impact of climate change on wheat production and providing solutions to adapt to it by considering the uncertainty of AOGCM models and greenhouse gas emission scenarios in order to increase food security (case study: Khuzestan plain). PhD thesis on irrigation and drainage, University of Shahid Chamran Ahvaz.

FAO, (2007). Adaptation to climate change in agriculture, forestry and fisheries: Perspective, framework and priorities. Interdepartmental Working Group on Climate Change. Rome. Available on: <http://www.fao.org>

Hamed, M. M., Nashwan, M. S., Shahid, S., Wang, X. J., Ismail, T. B., Dewan, A., & Asaduzzaman, M. (2023). Future Köppen-Geiger climate zones over Southeast Asia using CMIP6 Multimodel Ensemble. *Atmospheric Research*, 283, 106560.

Khosravi, M. & Aramesh, M. (2011). Climatic zoning of Central province using factor-cluster analysis. *Journal of Geography and Environmental Planning*, 23(2), 87-100.

Kilsby, C.G., Jones, P.D., Burton, A., Ford, A.C., Fowler, H. J., Harpham, C., & Wilby, R. L.

(2007). A daily weather generator for use in climate change studies. *Environmental Modelling & Software*, 22(12), 1705-1719.

Mohammadlu M., & Tahmasbipour, N. (2017). Assessment of the effects of climate change on climate classifications in parts of northwestern Iran. *Rainwater catchment systems*. 5 (4), 35-46.

Peel, M. C., Finlayson, B. L., & McMahon, T. A. (2007). Updated world map of the Köppen-Geiger climate classification. *Hydrology and earth system sciences*, 11(5), 1633-1644.

Rahimi, J., Laux, P., & Khalili, A. (2020). Assessment of climate change over Iran: CMIP5 results and their presentation in terms of Köppen-Geiger climate zones. *Theoretical and Applied Climatology*, 141, 183-199.

Semenov, M. A., & Barrow, E.M. (1997). Use of a stochastic weather generator in the development of climate change scenarios. *Climatic change*, 35(4), 397-414.

Soltani, A., & Hoogenboom, G. (2003). Minimum data requirements for parameter estimation of stochastic weather generators. *Climate Research*, 25(2), 109-119.

Taghavi, F., Naseri, M., Bayat, B., Metolian, S. S., & Azadi Fard, D. (2013). Determination of climate behavior patterns in different regions of Iran based on spectral analysis and clustering of extreme values of precipitation and temperature. *Natural Geography Research*, 77 (43), 109-124.

Taseh, M. & Barimani, F. & Ismail Nejad, M., (2017). Climatic zoning of Sistan and Baluchistan province. *Journal of Geography and Development*, 6(12), 101-116

Zarenistanak, M., Dhorde, A.G., & Kripalani, R.H. (2014). Temperature analysis over southwest Iran: trends and projections. *Theoretical and applied climatology*, 116(1-2), 103-117.

